MATERIALS CHEMISTRY FRONTIERS

RESEARCH ARTICLE

View Article Online
View Journal | View Issue

Cite this: *Mater. Chem. Front.*, 2023, **7**, 1374

Sulfur–oleylamine copolymer synthesized *via* inverse vulcanization for the selective recovery of copper from lithium-ion battery E-waste†

Suchithra Ashoka Sahadevan, [a] Xiong Xiao, [b] Yiqian Ma,[c] Kerstin Forsberg, [c] Richard T. Olsson [b] and James M. Gardner [a]*

Elemental sulfur (S_8) is an abundant and inexpensive by-product of petroleum refining. Polymeric sulfur is thermodynamically unstable and depolymerizes back to S_8 with time, which limits its applications and causes megatons of sulfur to accumulate in nature. A novel sulfur–oleylamine copolymer, synthesized using the inverse vulcanization method, is reported for the selective recovery of Cu^{2+} from a complex mixture of transition metals. Adsorption studies have been performed using batch experiments in the simulated aqueous solution containing a mix of metal ions (M^{x+} = Fe, Al, Mn, Co, Ni and Cu). The effect of different adsorption parameters such as pH, time, adsorbent dose, sulfur content, and desorption have been studied. The results demonstrate that the sulfur–oleylamine copolymer shows high selectivity towards Cu^{2+}, with excellent adsorption efficiency of >98% in acidic pH (pH ≈ 1) at room temperature, which is of practical relevance in the handling of battery leach liquors obtained from industrially derived blackmass. Finally, the sulfur–oleylamine copolymers were also applied to battery leach liquors with hydrochloric (HCl) or citric acid and showed Cu^{2+} adsorption efficiency of >98% ± 1 and > 95% ± 7, respectively. This work presents a novel way to convert industrial waste into a stable sulfur polymer and demonstrates its use as a promising material for selective recovery of Cu ions from battery waste and industrial effluents in a simple and cost-effective manner.

Received 27th October 2022,
Accepted 15th February 2023

DOI: 10.1039/d2qm01093c

rsc.li/frontiers-materials

1. Introduction

The demand for lithium-ion battery (LiB) containing electric vehicles and electronic goods has rapidly increased over the past few decades. While humanity has benefited immensely from these new goods and technologies, the disposal of this electronic waste (or e-waste) is one of the fastest-growing global concerns.[1,2] According to the 2020 UN Global E-waste Monitor, 53.6 million tonnes (Mt) of global e-waste was generated in 2019, and it is forecast to rise to 74 Mt by 2030.[3] Of that, 11 Mt are expected to be LiB waste alone. The accumulation of LiB e-waste can be both a severe threat to environmental health and potentially a rich source of valuable metals such as lithium (Li), cobalt (Co), copper (Cu), and nickel (Ni). The most widely used battery recycling method is hydrometallurgy.[4,5] The metal composition in LiB waste dramatically varies depending on the type and manufacturers of LiB and is typically Co 5–20%, Ni 0–10%, Li 5–12%, Al 3–10%, Fe 0–25%, Mn 5–12%, and Cu 7–17%.[6,7] Among these metals, Li, Co, and Ni, are considered the most valuable metals, and the rest of the metals (Fe, Al, and Cu) are often considered impurities. Fe and Al impurities are selectively removed by precipitation by adjusting the pH of the solution between 3.5–5.5. Eric *et al.* used a simple and low-cost precipitation method to remove almost 99% Cu impurities by adjusting pH to 6.47.[8] However, selective precipitation of Cu was challenging as a significant amount of Mn, Ni, and Co were co-precipitated. Hence, new methods to selectively separate specific metal ions for cost-effective and facile extraction are always sought. Other Cu removal methods from LiB waste include solvent extractions, electrodeposition, or ion exchange.[8–10] Peng *et al.* reported Cu removal from LiB waste using a multi-step process: electrodeposition followed by the extraction of the remaining Cu using N902 organic extractant.[10] However, current Cu removal methods from LiB waste are either expensive, multi-step complicated processes, or methods with low selectivity. At the same time, Cu is an essential element for body functions; however, excess Cu can cause severe damage, such as Parkinson's

[a] *Department of Chemistry, Division of Applied Physical Chemistry, KTH Royal Institute of Technology, Teknikringen 30, SE-100 44, Stockholm, Sweden. E-mail: jgardner@kth.se*
[b] *Department of Fibre and Polymer Technology, KTH Royal Institute of Technology, Teknikringen 56, SE-100 44, Stockholm, Sweden*
[c] *Department of Chemical Engineering, KTH Royal Institute of Technology, Teknikringen 42, 11428 Stockholm, Sweden*

† Electronic supplementary information (ESI) available. See DOI: https://doi.org/10.1039/d2qm01093c

and Alzheimer's diseases.[11] According to the U.S. Environmental Protection Agency (EPA), the safe limit of Cu content in drinking water is 1.3 ppm.[12] Hence, methods to remove heavy metal ions like Cu are also important in water handling and from an overall environmental perspective.

Sulfur is an abundant industrial by-product from petroleum refineries and natural gas production, with a reported production of close to 70 Mt per year.[13] Although elemental sulfur is processed into bulk chemicals such as sulfuric acid and fertilizers, the supply of sulfur as a raw material drastically exceeds demand and often causes megaton stockpiles.[14,15] Thus, utilization of this inexpensive elemental sulfur as a raw material to a value-added material is of great interest to overcome the ''excess-sulfur problem''. The elemental sulfur, S_8, can be heated above 159 °C to undergo ring-opening polymerization to form polymeric sulfur. However, this process is reversible; and depolymerization to S_8 occurs at room temperature, making it challenging to find applications for this sulfur chemistry. In 2013, Pyun and co-workers introduced crosslinked sulfur polymers as a new class of polymers prepared by inverse vulcanization.[15,16] In this method, a crosslinker is added to the diradical polymeric sulfur to undergo free radical polymerization and form a stable sulfur polymer at room temperature.[17] Depending on the intended use, the choice of crosslinker and the quantity of sulfur can be used to modify or tune the morphology and properties of the crosslinked sulfur polymer. A wide range of sulfur polymers based on different crosslinkers, such as limonene,[18,19] styrene, fatty acid derivatives like vegetable oil, canola oil, *etc.*,[20] are reported and explored for other fields such as optics fertilizers and as components in solar cells, *etc.*[14,21–29] Moreover, sulfur is a soft Lewis base; considering (Hard–Soft–Acid–Base) HSAB theory, the sulfur polymer can be exploited to form covalent bonds with soft Lewis acids; hence it has been receiving significant attention in recent years with heavy metal sorption.[22] For example, sulfur–canola oil copolymer is one such material that has mainly been studied for the recovery of heavy metal ions such as Hg, Au and Fe.[28,30–33]

In this work, a sulfur–oleylamine copolymer has been synthesized and evaluated for the selective recovery of Cu from battery and e-waste. Oleylamine is an organic ligand that has been studied in nanoparticle synthesis as a capping agent, solvents, surfactants, and reducing agents.[34–36] It is sustainable and cheaper than commercially available pure alkylamine, stable at high temperatures and the presence of alkene group in the oleylamine can undergo free-radical polymerization, making it a feasible crosslinker for inverse vulcanization. Adsorption studies have been performed for aqueous solutions containing six mixed metal ions of relevance in the recycling of LiB such as Fe, Al, Mn, Co, Ni and Cu and the effect of different adsorption parameters such as pH, time, adsorbent dose, sulfur content, and desorption are studied. Finally, the sulfur–oleylamine copolymer was used as a sorbent to recover Cu ions from true battery leach liquor solutions. To the best of our knowledge, this is the first sulfur copolymer with selective binding to copper. As the sorbent preparation is facile, cheap, solvent-free and feasible to produce in large scale quantities, this material is a potential candidate to use in real practical applications.

2. Experimental

2.1. Materials and methods

All the chemicals were purchased from Sigma-Aldrich, Sweden, and used without further purification. Technical grade of elemental sulfur, oleylamine (70%) and analytical grade of metals salts (≥98%) such as $CoCl_2{\cdot}6H_2O$, $NiCl_2{\cdot}xH_2O$, $Al_2NO_3{\cdot}9H_2O$, $CuCl_2$, $FeCl_2$, $MnCl_2{\cdot}4H_2O$, citric acid, hydrochloric acid (37%), nitric acid (65%) and ICP-OES standard solutions of 1000 mg L^{-1} for Fe, Mn, Ni, Cu, Co, and Al in 2–5 wt % HNO_3. Deionized water was used for the sample preparation. Battery waste as a black mass was supplied from Volvo Cars AB, Sweden and was used without any further pre-treatment. Black mass is obtained after mechanical pre-treatment, discharging and shredding.

2.2. Synthesis

Sulfur–oleylamine copolymer was prepared by inverse vulcanization method according to the previously reported literature with a slight modification (Scheme 1).[16]

Sulfur-50%-oleylamine copolymer or poly(S-50%-OA) (10 g scale). 5 g of elemental sulfur was added to 180 °C preheated 30 ml vial fitted with a magnetic stirrer at 700 rpm. After a couple of minutes, the sulfur completely melted and turned from a yellow easily flowing liquid to an orange, syrupy, viscous liquid. To the melted sulfur, 5 g oleylamine was added and allowed to stir for around 8 minutes. An immediate color change of the reaction mixture was observed from orange to dark brown. The solution was allowed to cool at room temperature, and the material was recovered by breaking the glass vial. Sulfur–oleylamine copolymer with different sulfur contents (wt %) 30% and 70% were prepared in a similar manner except that 3 g sulfur, 7 g oleyalmine and 7 g sulfur, 3 g oleylamine were used for poly(S-30%-OA) and poly(S-70%-OA) respectively. To have a homogeneous poly(S-50%-OA) for all the batch evaluation experiments, the polymer was prepared in a large scale, *i.e.* in 40 g in the same manner.

Leaching. Leaching experiments were performed with 3 N hydrochloric acid (HCl) and 1.5 M citric acid, according to the previously reported literature.[37,38] For the citric acid, ultrasound-assisted citric acid leaching was used for the effective extraction.

2.3. Adsorption experiments

Simulated metal solution. 25 mg L^{-1} of stock solution were prepared by dissolving metal chloride salts of Fe, Co, Mn, Ni, Cu and nitrate salt of $Al(NO_3)_3$ in deionized water. All the experiments were repeated a minimum of three times to ensure reproducibility.

Selectivity studies. Studies on selective adsorption of metal ions were conducted in simulated metal solutions containing six metal ions (M^{2+} = Fe, Co, Mn, Ni, Cu and Al) prepared in the laboratory. Batch experiments were conducted in a 30 mL vial

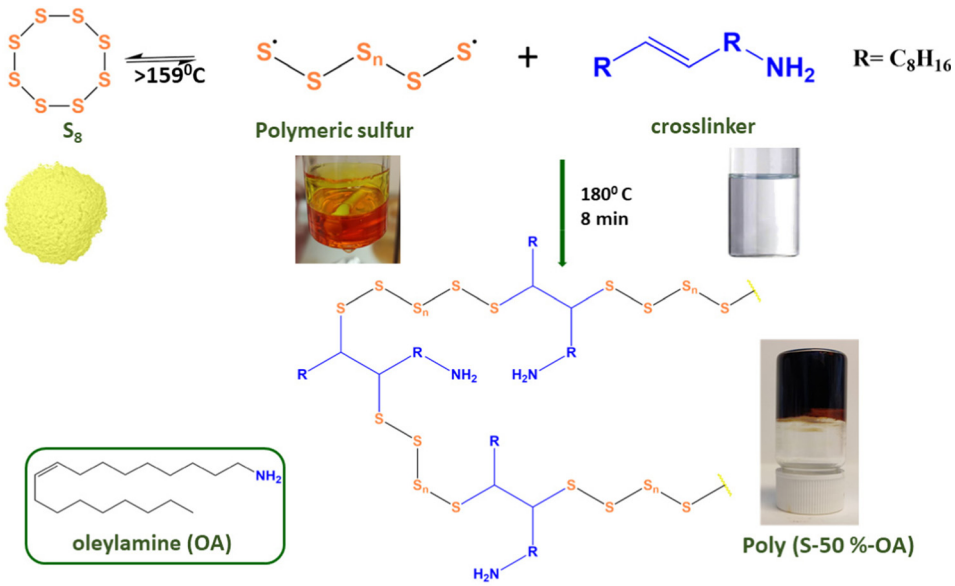

Scheme 1 Schematic illustration for the synthesis of poly(S-50%-OA). The structure of the crosslinker (oleylamine) is shown in the inset.

with 0.5 g poly(S-50%-OA) adsorbent in 20 ml solutions (25 mg L^{-1}) at room temperature for overnight stirring. After the treatment, the adsorbent was filtered, and the metal solution was centrifuged at 6000 rpm for 10 min. The concentration of metal ions in the supernatant was measured by inductively coupled plasma emission spectrometry (ICP-OES). Adsorption efficiency (%) was calculated as shown in eqn (1).

$$\text{Adsorption efficiency } (\%) = \frac{(c_i - c_f)}{c_i} \times 100 \qquad (1)$$

where c_i and c_f are the metal concentration (mg L^{-1}) before and after adsorption measured using ICP-OES, respectively.

The parameters such as the effects of pH, adsorbent dose, contact time, sulfur content, the impact of Cu concentration on the selective adsorption of metal ions were tested. The effect of pH was examined at a metal concentration of 25 mg L^{-1} in the pH range of 1 to 4 by adjusting the pH of the solution with HCl or NaOH. The pH values were recorded using a digital pH meter at RT. The influence of adsorbent dose was tested using three different adsorbent amounts from 0.1 g, 0.5 g and 1 g. The time optimization studies were performed in 100 mL metal solution (25 mg L^{-1}), and subsequently increasing the adsorbent dose to 2.5 g with continuous stirring for 10 h. 2 mL aliquots were collected every hours. The effect of Cu concentration was investigated by varying Cu concentration from 25, 50, 100 and 300 mg L^{-1}. Finally, the sulfur-copolymer was applied in battery systems.

Regeneration studies. The desorption studies were performed by collecting the sorbent after adsorption and soaking them in 1 N HCl with continuous stirring at RT for 6 h. The aliquot was collected, and the concentration was measured using ICP-OES.

Application in battery system. The leaching experiments were conducted in inorganic and organic leach liquors of HCl and citric acid. The selectivity studies of Cu were performed in 20 mL HCl and citrate leach liquors with 0.5 g poly(S-50%-OA). The leach liquors were diluted to make the initial concentration of Cu around 25 mg L^{-1}. The metal concentration before and after adsorption were analyzed using ICP-OES.

The adsorption parameters and conditions used for the selectivity studies are summarized in Table 1.

2.3. Characterization

Sulfur–oleylamine copolymer. ^{1}H NMR experiments were measured with a Bruker DMX-400 MHz spectrometer using $CDCl_3$ as a reference solvent. Powder X-ray diffraction (PXRD)

Table 1 Parameters and conditions used in the batch experiments for selectivity studies

Effect of adsorption parameters	Variants	Constant
pH	1, 2, 3, 4	25 mg L^{-1}, 20 mL metal solution at RT
Adsorbent dose (g)	0.1, 0.5, 1	25 mg L^{-1}, 20 mL metal solution at RT
Contact time (h)	1–10	25 mg L^{-1}, 100 mL metal solution at RT
Sulfur content (S wt%)	30, 50, 70	25 mg L^{-1}, 20 mL metal solution at RT
Cu concentration alone (mg L^{-1})	25, 50, 100, 300	20 mL Cu solution at RT
Battery system	HCl leach liquor Citric acid leach liquor	30 mg L^{-1} Cu concentration, 20 mL leach liquor at RT

*Metal solution = simulated stock solution of Fe, Mn, Co, Ni, Cu and Al

patterns of the polymer before and after adsorption were performed on X'Pert PRO, PANalytical using CuKα radiation (λ = 1.5406 Å) with a scan rate of 0.01 from 10–70°. Thermogravimetric analysis (TGA) was performed on a Mettler-Toledo TGA/SDTA851. The measurements were carried out under 50 mL min^{-1} nitrogen from 30 to 900 °C, with a heating rate of 10 °C min^{-1}. Scanning electron microscopy (SEM) was performed in Hitachi S-4800 instrument. SEM images were taken at an acceleration voltage of 1 kV and a current of 10 mA. Sputtering of the samples was performed for 20 s using a Cressington 208HR, equipped with a Pt/Pd target. The composition of metals in the sorbent after adsorption were measured using Energy-dispersive X-ray spectroscopy (EDS), carried out at 15.0 kV. Attenuated total reflectance Fourier transform infrared spectroscopy (ATR-FTIR) of solid samples were recorded using PerkinElmer spectrometer in the range of 4000–400 cm^{-1}. The intrinsic viscosity [η] was measured by capillary solution viscometry. The poly(S-50%-OA) sample was dissolved in tetrahydrofuran (THF) at four different concentrations. A LAUDA iVisc Capillary Viscometer equipped with an Ubbelhode viscometer was used to record the flow-through time at 23 ± 0.1 °C.

Metal solutions. The concentration of metal solutions was determined using ICP-OES (Thermo Fisher iCAP 7400, USA). All the metal solutions were diluted with 5 wt% HNO_3 into suitable metal concentration ranges for the ICP-OES.

3. Results and discussion

3.1. Synthesis of sulfur–oleylamine copolymer

Sulfur–oleylamine copolymer is synthesized by inverse vulcanization between sulfur and the crosslinker, oleylamine. Elemental sulfur transforms into a polymeric radical by a ring opening polymerization reaction at temperatures above 159 °C. The unsaturated bond in the oleylamine reacts with the radical sulfur polymers to form a free radical that further reacts with sulfur radicals to form a crosslinked polymeric sulfur, namely poly(S-*r*-OA). Depending on the amount of sulfur (wt%), r varies from 30, 50 and 70. The polymer is allowed to cool to form hard glassy material, which are broken to smaller particles using hammer and then used for adsorption studies. Contrary to commonly known sulfur copolymers especially with fatty acid derivatives, the poly(S-50%-OA) is soluble in wide range of organic solvents (Fig. S1, ESI†), probably due to the presence of amine group in the material and absence of unsaturated groups. More often, the poor solubility of other crosslinked sulfur polymers is related to increase in unsaturation or

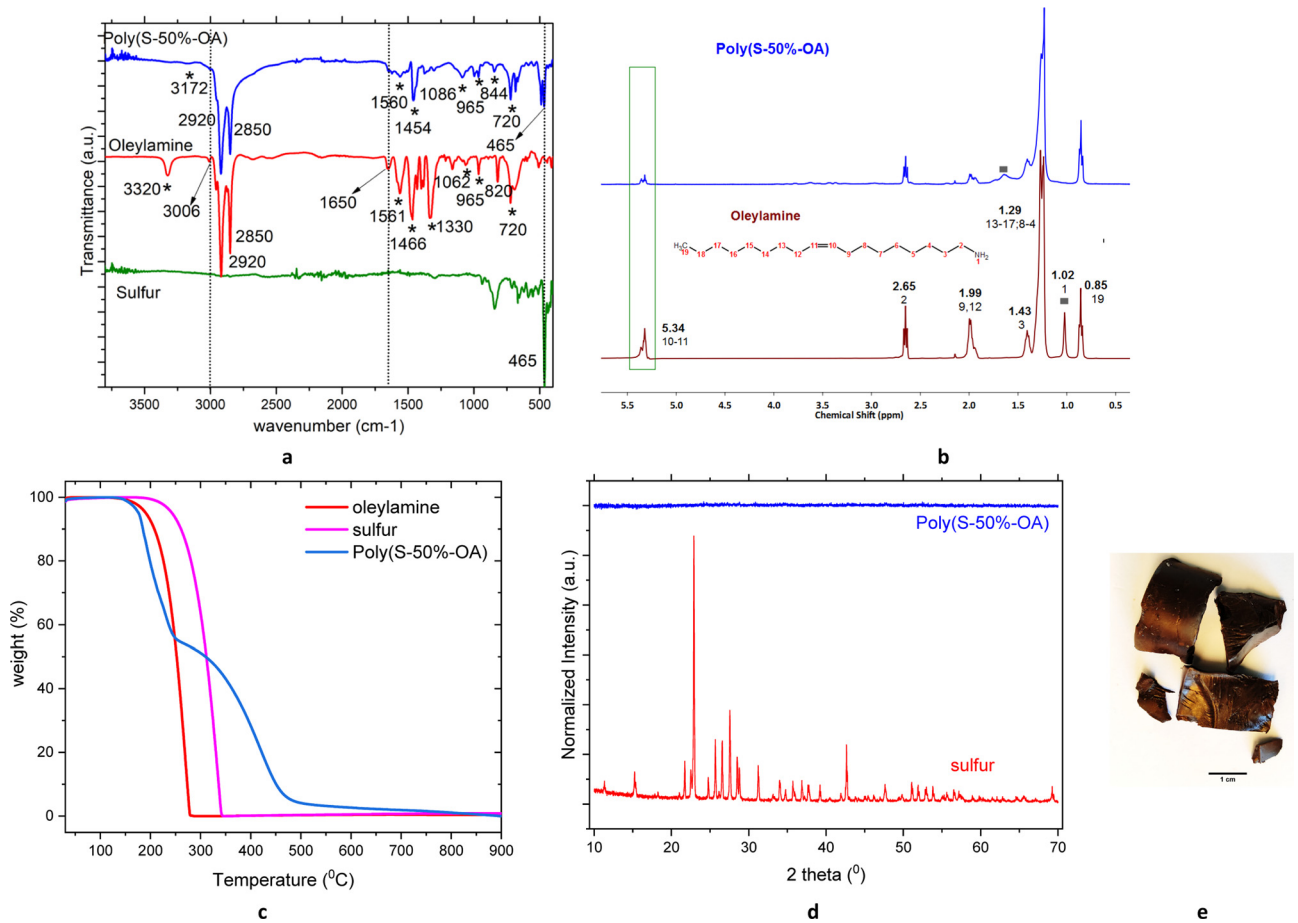

Fig. 1 Characterization of poly(S-50%-OA) (a) AT-FTIR (b) ^{1}H-NMR (c) TGA (d) PXRD (e) photograph of the material.

number of vinylic groups in the monomer and high degree of crosslinking.[25]

3.2. Characterization of sulfur–oleyalmine copolymer

The AT-FTIR spectrum of poly(S-50%-OA) compared to oleylamine shows the weakening of alkene C–H and C═C stretching vibrations at 3010 and 1650 cm^{-1} respectively, which reveals the cleavage of C═C bond and successful copolymerization of oleylamine with sulfur.

The polymer shows two strong characteristic vibrational modes of alkyl group at 2920 and 2850 cm^{-1}, corresponds to C–H_2 symmetric and asymmetric stretch respectively. Additionally, peaks around 1460 cm^{-1} corresponds to C–H bending mode. The peak at 965 cm^{-1} in oleylamine corresponds to C═C bending mode, while this peak has weekend in the polymer is additional evidence of polymerization through double bond opening. The peaks around 3320 and 1062 cm^{-1} in the free oleylamine, corresponds to N–H and C–N stretching respectively, while this peak is shifted to 3172 and 1086 cm^{-1} in the polymer, indicates some of the primary amine group from the oleylamine might be taking part in the reaction and have formed secondary amine (3350–3310 cm^{-1}). The peak at 720 cm^{-1} in both monomer and polymer corresponds to N–H bending (out of the plane) which suggests the presence of amine group in the polymer. Moreover, the presence of the peak at 465 cm^{-1} in poly(S-50%-OA) compound, corresponds to S–S stretching vibrations, which are consistent to other crosslinked sulfur polymeric materials (Fig. 1(a) and Fig. S2, ESI†). The vibrational modes of corresponding monomers and the polymers and their assignment are summarized in Table S1 (ESI†).[36,39,40] The crosslinking reaction is further supported by ^{1}H NMR of poly(S-50%-OA) copolymer in comparison with oleylamine monomer Fig. 1(b). The proton peak at δ 5.40 ppm corresponds to CH_2 protons from the alkene group and the decrease in magnitude of this peak in the poly(S-50%-OA) further validates the cleavage of C═C bond and a successful reaction. The proton peak of alkene shows doublet of doublet, which could be a result of *E*/*Z* isomerization, through the addition of a RS$^\bullet$ radical to the cis alkene, followed by β-elimination to form trans alkene.[41] The terminal methyl groups are present in the polymer around δ 0.85 ppm. However, there is a shift in amine proton peaks in the polymer from 1.06 ppm in monomer to 1.6 ppm, this behaviour is due to N–H resonance as reported in previous literatures[42] (denoted as grey rectangle in Fig. 1(b)). Moreover, intensity of amine peaks is further reduced, confirms the observation from AT-IR, that part of amines in oleylamine could be involved in the reaction. The thermal stability of the poly(S-50%-OA) was measured using TGA under N_2 atmosphere and shows that material has good stability till 140 °C and after that undergoes two-step degradation, as commonly seen for sulfur and oil-derivative copolymer.[25,31] The first decomposition may correspond to S–S bond breakage and the second step weight loss can be attributed to decomposition of organic contents (Fig. 1(c) and Fig. S3, ESI†).[23] The PXRD pattern of elemental sulfur (S_8) compared with poly(S-50%-OA) is shown in Fig. 1(d), indicates the conversion of crystalline sulfur to amorphous copolymer, as observed by naked eye (Fig. 1(e)). As explained in the ESI,† the approximate molecular weight of the poly(S-50%-OA) was calculated to be *ca.* ∼18 kDa using the Mark–Houwink–Sakurada (MHS) equation following the intrinsic viscosity measurements.

3.3. Selectivity of metal ions

Batch experiments on the selectivity of poly(S-50%-OA) towards Cu^{2+} metal ions were studied in the simulated metal solution at concentration around 25 mg L^{-1}. Poly(S-50%-OA) was stirred overnight forming brown suspension (Fig. 2(a)) and pH of the solution increased from 4 to 5. Interestingly, poly(S-50%-OA) shows high selectivity towards Cu^{2+} ions and the concentration of Cu^{2+} was significantly reduced from 27 mg L^{-1} to less than 3 mg L^{-1} (Fig. 2(b)).

On the basis of Hard–Soft–Acid–Base (HSAB) theory, the selectivity can be attributed to the coordination sulfur and Cu^{2+}, a soft base and soft acid, respectively. The concentrations

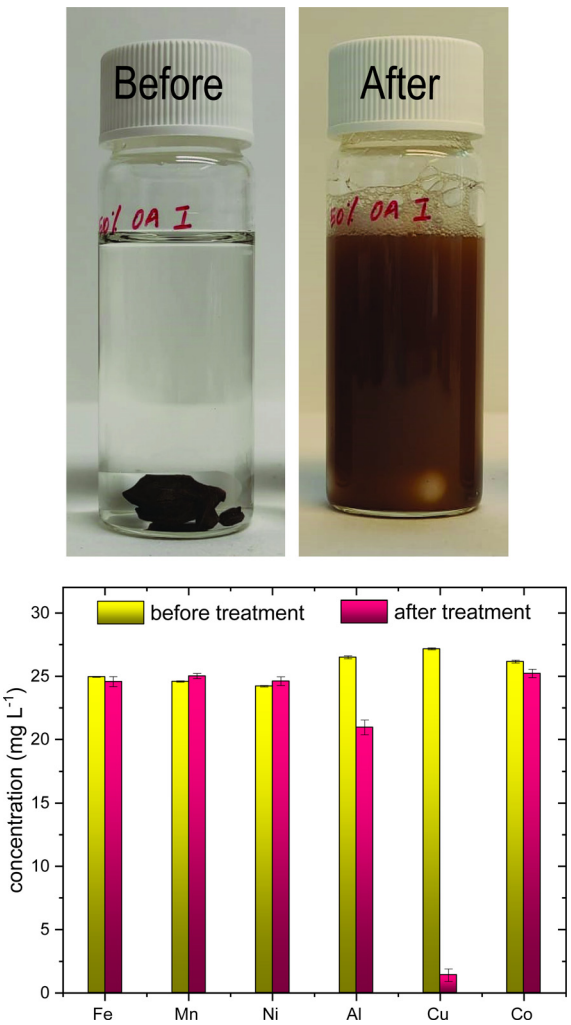

Fig. 2 (a) Photograph of batch experiment on selectivity studies before and after adsorption. (b) Metal selectivity profile in terms of concentration (mg L^{-1}) before and after adsorption.

Table 2 Initial and final concentration of metal solution before and after adsorption

	Fe	Mn	Co	Ni	Cu	Al
C_i mg L^{-1}	24.96	24.59	26.16	24.22	27.17	26.51
Std dev	0.04	0.53	0.11	0.06	0.08	0.11
C_f mg L^{-1}	24.6	25.02	25.23	24.62	1.5	20.96
Std dev	0.4	0.2	0.33	0.34	0.5	0.58

C_i – initial concentration; C_f – final concentration

of the other metal ions before and after adsorption are shown in Table 2.

SEM images of the adsorbent before and after adsorption demonstrate a change in morphology of the material. The morphology of the poly(S-50%-OA) copolymer before adsorption shows relatively homogeneous and amorphous surface, whereas after adsorption the polymer shows the presence of preferential growth and crystallinity (Fig. 3(a) and (b)). The EDX mapping in the adsorbent after adsorption showed the presence of sulfur and carbon, however Cu content in the region was relatively low, which could be due to the lower mass concentration of Cu compared to sulfur (25 mg L^{-1} Cu and 500 mg adsorbent) (Fig. S6, ESI†). Hence, Cu concentration was increased from 25 mg L^{-1} to 300 mg L^{-1}, without other metal ions, SEM image and crystallinity was consistent like in previous, with lower concentration. The EDX mapping after the adsorption showed the presence of S, C and Cu content. The crystalline region corresponds to sulfur (yellow region), the presence of Cu on the surface was almost uniform, irrespective of the S concentration (red) (Fig. 3(c)). PXRD results from the poly(S-50%-OA) polymer after adsorption complements the evidence from SEM-EDX result. In comparison with the PXRD of adsorbent before adsorption, it has more crystalline peaks although weakly diffracting, and which corresponds to sulfur PXRD pattern (Fig. 1(d) and 3(d)).

The AT-FTIR transmittance spectra of the adsorbent measured after adsorption is shown in Fig. 4. The AT-FTIR spectra shows the presence of new peaks especially in the fingerprint region, at lower wavenumber <1500 cm^{-1}. At the higher wavenumber, in the range between 3500–1800 cm^{-1}, there is no noticeable change, as that region mainly consist of alkyl stretching vibrations. The presence of new peak in the region between 1070–1000 cm^{-1} and below 500 cm^{-1} can be interpreted to Cu–S vibration, confirming Cu–S coordination (pink shaded region).

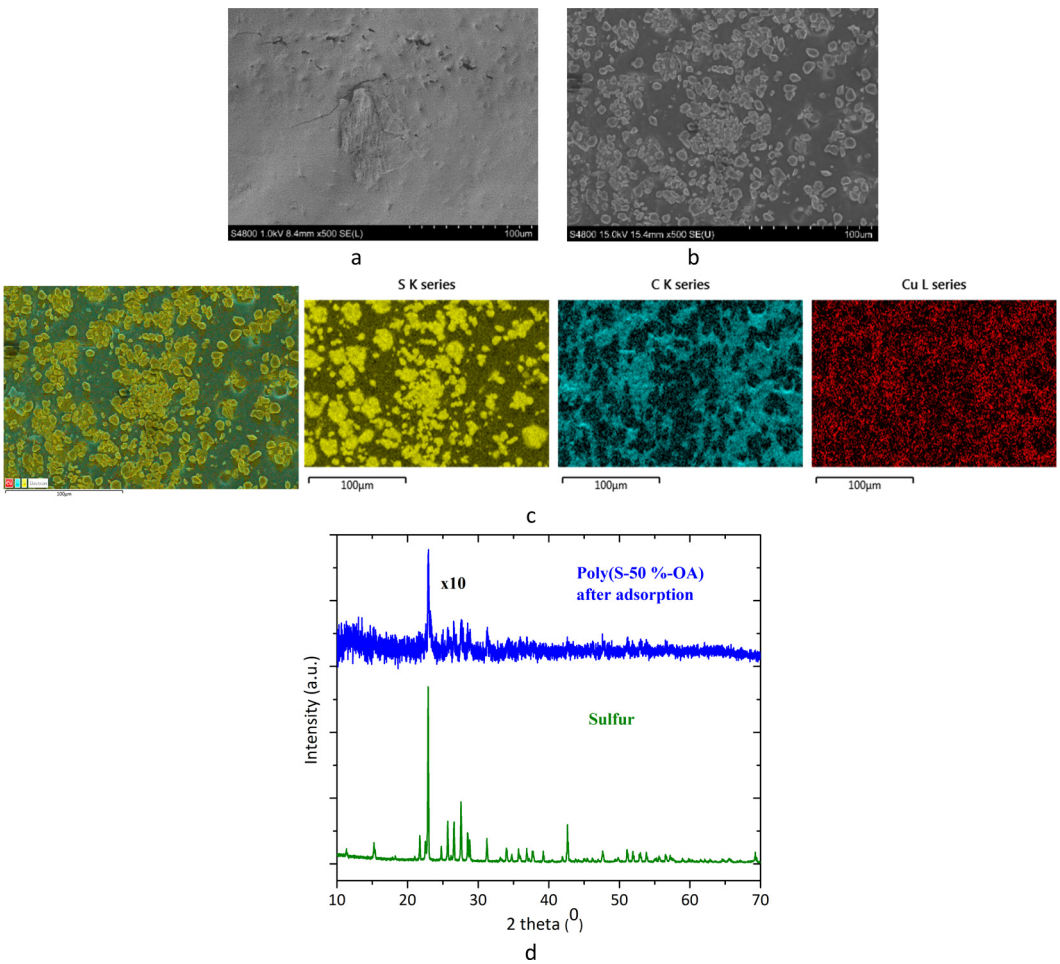

Fig. 3 SEM image of poly(S-50%-OA) (a) before adsorption (b) after adsorption (c) EDX mapping of poly(S-50%-OA) after adsorption (d) PXRD of poly(S-50% OA) after the adsorption.

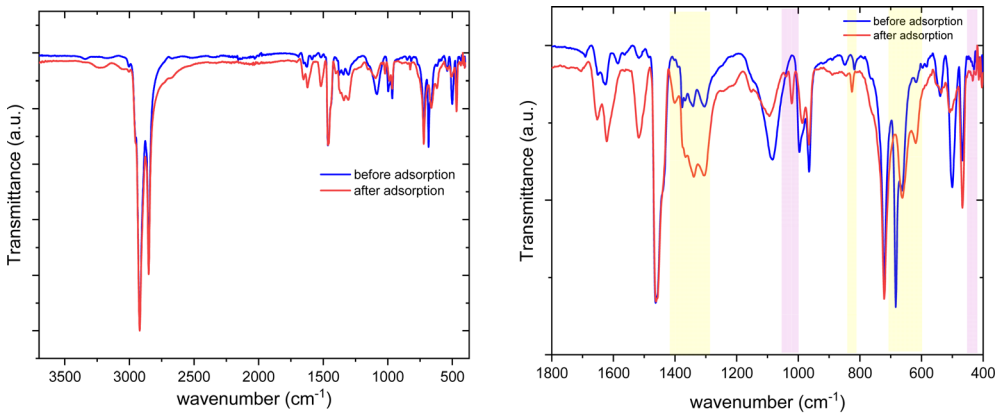

Fig. 4 ATR-FTIR spectra of poly(S-50%-OA) before and after adsorption (a) 3700–400 cm^{-1} (full spectra) (b) zoom spectra in the fingerprint region.

There is a shift of almost 10 cm^{-1} for the peaks in the region between, 850–800 cm^{-1} and at 685–675 cm^{-1} that corresponds to changes in C–S vibration due to the metal coordination (yellow shaded region). Several parameters were studied on simulated aqueous metal solutions including: the effect of the initial pH, adsorbent dose, contact time, sulfur content, and the effect of Cu concentration alone on the selective adsorption of Cu.

Effect of initial pH. The pH of the leach liquor is an important parameter for the selectivity, adsorption and desorption of metal ions. The influence of pH on the adsorbent upon selective adsorption of Cu is studied by varying pH between 1–4. Acidic pH were chosen as they are ideal for most of the industrial applications such as battery leach liquors and industrial effluents, moreover, at pH >5, metal species such as $Fe(OH)_3$ and $Al(OH)_3$ starts to precipitate. The effect of pH on adsorption efficiency is presented in Fig. 5. Interestingly, adsorption efficiency increases with decreasing pH. For initial pH, at 1, Cu was selectively adsorbed with an adsorption efficiency of nearly 100%. However, in the overall pH range between 1–4, Cu was selectively adsorbed with efficiency greater than 80–90%. These data suggest that adsorption is primarily through the coordination of sulfur and Cu, which ought to be independent of pH. For most experiments the stock solution had a pH of 4. During adsorption, the pH of the solution increases from 4 to 5 and along with Cu some Al is also removed (<20%).

Effect of contact time. The influence of contact time on the selective adsorption of Cu was investigated. Fig. 6 shows the effect of adsorption efficiency over time. The adsorption efficiency increased rapidly in the beginning, almost 70%, over 2 h. The adsorption rate decreases slowly after that and reaches a plateau (>90%) after 5 h, as adsorption reaches an equilibrium.

Effect of sulfur content, adsorbent dose and Cu concentration. Sulfur–oleylamine copolymers were prepared with varying sulfur content (30, 50, 70 wt%) and adsorption experiments were carried out in the same experimental setup. The color of the solution turned to brown after the overnight stirring. (Fig. S4, ESI†). It was also observed that pH of the supernatant change from 4 to 5. In all the cases, Cu was selectively adsorbed with adsorption efficiency more than 90%, some amount of Al was also adsorbed (20–30%). However, there was no noticeable

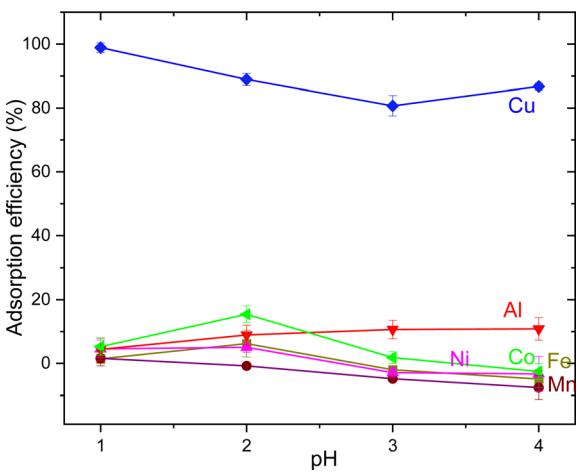

Fig. 5 Adsorption efficiency of metal ions at varied pH.

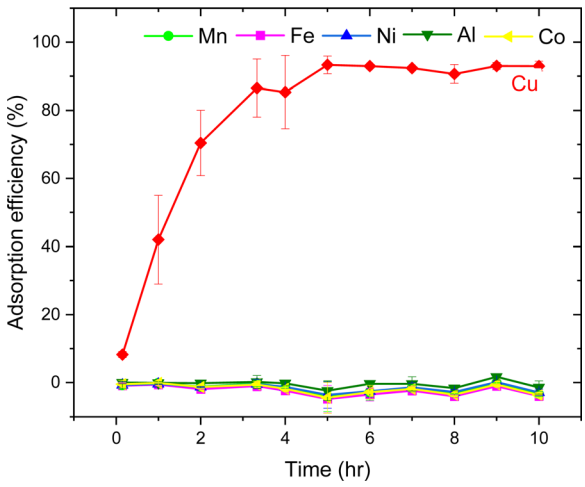

Fig. 6 Adsorption efficiency of metal ions over the period of time.

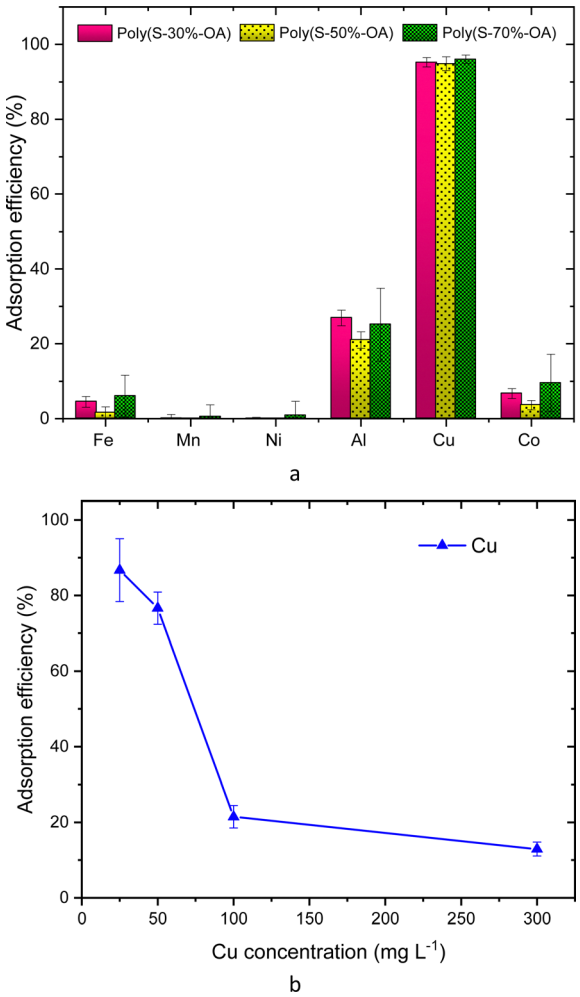

Fig. 7 Adsorption efficiency of metal ions with varying (a) sulfur content in poly(S-*r*-OA) (*r* = 30, 50, 70 wt%) (b) Cu concentration (mg L^{-1}) in solution using 0.5 g poly(S-50%-OA) adsorbent.

change in the adsorption efficiency of Cu with increasing sulfur content and remain relatively constant, 95% ± 1.23, 94.8% ± 1.83 and 96.03% ± 1.11 for 30, 50 and 70 wt% sulfur respectively (Fig. 7(a)). This can be probably due to the low concentration of metal ions and the presence of more available active sites. It was confirmed by increasing the copper concentration from 25, 50, 100 and 300 mg L^{-1}, without other metal ions, and for the same amount of adsorbent quantity, the adsorption efficiency was found to be decreasing (Fig. 7(b)). For instance, at higher concentration, 300 mg L^{-1}, adsorption efficiency gets reduced to <20%, due to the non-availability of accessible active sites as it reaches the saturation. The SEM-EDX mapping of adsorbent after the treatment with 300 mg L^{-1} Cu solution shows the presence of both S and Cu (Fig. 3).

Effect of adsorbent dose. The influence of adsorbent concentration on the selective adsorption of Cu was investigated at an initial metal concentration of 25 mg L^{-1} for sulfur-copolymer dose ranging from 0.1, 0.5 and 1 g. As expected, adsorption efficiency increases with increasing adsorbent dose, due to the increasing active site available for adsorption. When the

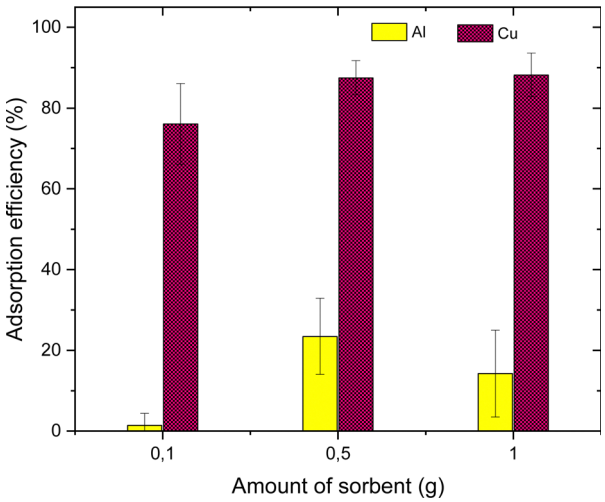

Fig. 8 Adsorption efficiency of metal ions with different adsorbent dose of poly(S-50%-OA).

adsorbent dose is 0.1 g, the adsorption efficiency was 76% ± 10, further increases above 85% for 0.5 g and a slight improvement was observed for a 1.0 g adsorbent dose (Fig. 8).

Desorption studies. The regeneration or desorption studies on the polymer were performed by treating the adsorbent collected after adsorption with 1 N HCl for 6 h. All the metal ions except Cu^{2+} were successfully regenerated, which indicatives physisorption or electrostatic interactions between the negatively charged polymer (sulfide) and the positively charged metal ions (Fig. 9). On the other hand, Cu is not regenerated, which suggests that Cu is chemically bound or chemisorbed to the polymer. As Cu–S coordination is stable, it is possible that a mild reductant or oxidant could be added as an alternative to weaken sulfur and copper interactions. Further investigation is necessary to have deeper insights on the regeneration of the adsorbent and recovery of Cu as value-added materials such as copper sulfide or copper sulfate.

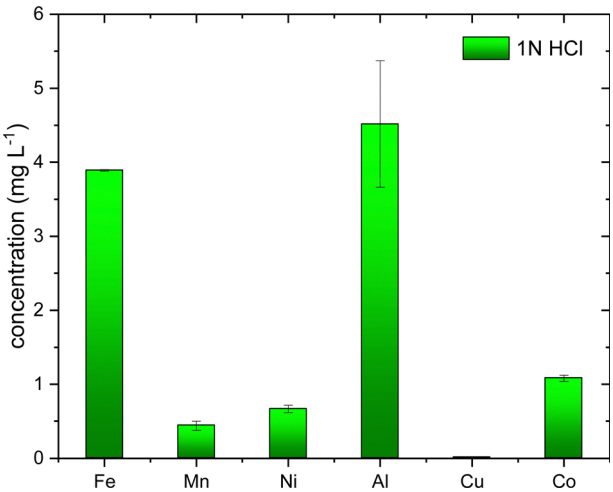

Fig. 9 Desorption/regeneration of metal ions after treating poly(S-50%-OA) recovered after adsorption in 1 N HCl for 6 h.

Applications in battery recycling. The laboratory simulated mixed metal aqueous solution was used to study the effect of each parameter on selectivity and adsorption efficiency. For practical applications in hydrometallurgical battery recycling, poly(S-50%-OA) were tested in both inorganic and organic leach liquor solution such as HCl and citric acid, respectively. Despite the fact that HCl is corrosive, it has still been used as an alternative to H_2SO_4–H_2O_2, due to the easier separation of metal ions such as Co, Ni and Mn at further extraction steps, which is more difficult in H_2SO_4 medium and potentially dangerous given that H_2O_2 can be explosive.[37] Another alternative for the inorganic acid is the environmentally friendly organic acids, such as citric acid. Recently, in 2021, energy-efficient and eco-friendly extraction of metal ions using citric acid and acetic acid assisted with ultrasound were reported by some of us.[38] As further advancement, selective extraction of metal ions from leach liquor are performed.

The initial Cu concentration in the leach liquor was made almost constant (30 mg L^{-1}) in the both the solutions, by diluting with deionized water and 0.5 g polymer were used with overnight stirring. In HCl leach liquor, Cu is selectively adsorbed with efficiency $>98\% \pm 1$, whereas in citric acid leach liquor, slight amount of $Fe^{2+/3+}$ and Al^{3+} are also adsorbed along with Cu with adsorption efficiency, $52\% \pm 12$, $40\% \pm 17$ and $>95\% \pm 7$ for $Fe^{2+/3+}$, Al^{3+} and Cu^{2+} respectively (Fig. 10). This difference in adsorption in two leach liquors can be speculated as mainly arising due to the difference in pH in both the solutions, as citric acid is weaker acid than HCl. Citric acid is also a good chelating agent, due to the presence of three carboxylate groups, citrate is known to form variety of coordination complexes with Fe and Al, even at acidic conditions.[43] However, it would an early stage to comment more about the difference in selectivity, as initial concentration of Fe and Al are quite low in the leach liquor. The results suggest the utility of sulfur–oleylamine copolymer as a selective adsorbent for Cu^{2+} ions, especially at acidic environment, and could be used for the industrial application in battery recycling or industrial effluents. Further investigations are necessary to confirm the conditions relevant for real world use such as polymer regeneration, effects of temperature, and polymer surface area to help improve the adsorption capacity.

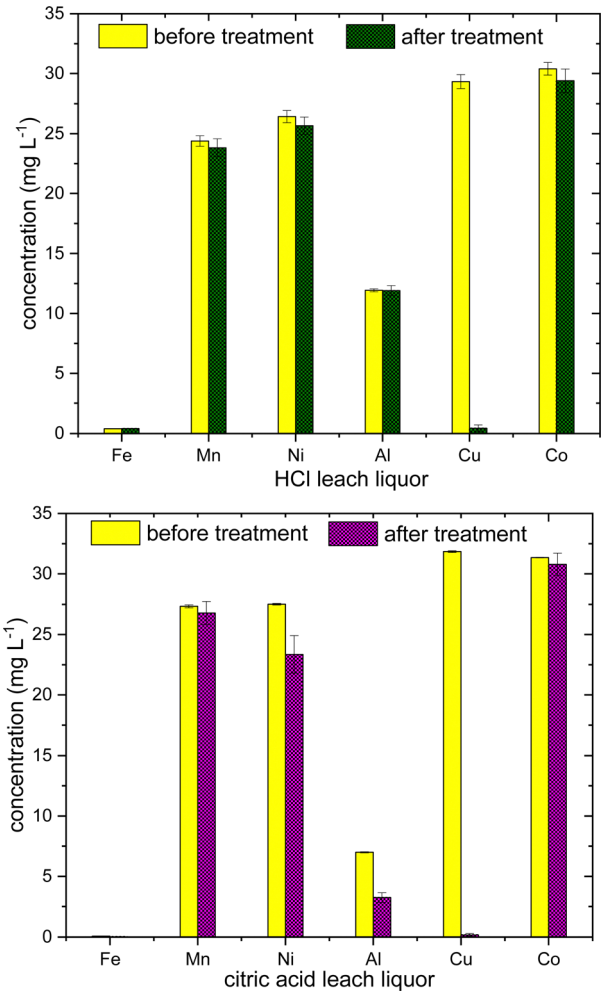

Fig. 10 Metal selectivity profile of poly(S-50%-OA) treated in HCl and citric acid leach liquor in terms of concentration (mg L^{-1}) before and after adsorption. Initial concentration of Cu^{2+} ion was diluted to 30 mg L^{-1}.

4. Conclusions

Poly(S-50%-OA) is synthesized using the inverse-vulcanization method and selective adsorption towards Cu^{2+} has been demonstrated from the mixed metal ions such as Fe, Al, Mn, Co, Ni and Cu. The selectivity is attributed to the interaction or coordination between sulfur and Cu^{2+} according to Hard–Soft–Acid–Base (HSAB) theory. Different parameters such as effect of pH, adsorbent dose, time, effect of sulfur content, effect of initial Cu concentration and desorption studies were also studied on selectivity and adsorption efficiency towards Cu^{2+}. The polymer shows high selectivity towards Cu^{2+} at acidic pH 1 with adsorption efficiency of $>98\%$, which is ideal for industrial applications, mainly for hydrometallurgical battery recycling processes, as this process mainly proceeds through leaching, involving acidic solutions and for the effluents. All the other metal ions adsorbed along with excepts Cu^{2+}, although small quantities, were successfully regenerated, suggests that it is physisorption for all other metals besides Cu^{2+}. On the other hand, Cu^{2+} is not regenerated, which implies that Cu^{2+} is chemically adsorbed or chemisorbed.

Poly(S-50%-OA) was also applied as an adsorbent towards selective adsorption of Cu^{2+} from true battery leach liquors, such as HCl and citric acid. The initial Cu concentration in both the leach liquor were made almost the same (30 mg L^{-1}) and the adsorption experiments were performed. In both HCl and citric acid leach liquor, Cu^{2+} is selectively adsorbed with efficiency $>98\% \pm 1$ and $>95\% \pm 7$ respectively.

The reported novel sulfur–oleylamine co-polymer could be a promising remediation to selectively recover Cu^{2+} ions from mixture of metal ions. The advantages of facile and green synthesis of sorbent preparation and low-cost economic benefits due to excess availability of raw material and the high

selectivity of sorbent towards Cu metal ions in acidic pH can make this material a good value for real practical applications such as in battery recycling and waste-water treatment.

Conflicts of interest

There are no conflicts to declare.

Acknowledgements

PERLI (Processes for Efficient Recycling of Lithium-ion Batteries) project 48228-1 granted by the Swedish Energy Agency is acknowledged for financial support. We would like to thank Assoc. Prof. M. Petranikova at Chalmers University of Technology for helping us to obtain battery blackmass from Volvo C30 (Swedish Energy Agency grant: 48204-1).

References

1 W. Li and V. Achal, Environmental and Health Impacts Due to E-Waste Disposal in China – A Review, *Sci. Total Environ.*, 2020, **737**, 139745.
2 R. Nithya, C. Sivasankari and A. Thirunavukkarasu, Electronic Waste Generation, Regulation and Metal Recovery: A Review, *Environ. Chem. Lett.*, 2021, **19**, 1347–1368.
3 L. Andeobu, S. Wibowo and S. Grandhi, An Assessment of E-Waste Generation and Environmental Management of Selected Countries in Africa, Europe and North America: A Systematic Review, *Sci. Total Environ.*, 2021, **792**, 148078.
4 F. Arshad, L. Li, K. Amin, E. Fan, N. Manurkar, A. Ahmad, J. Yang, F. Wu and R. Chen, A Comprehensive Review of the Advancement in Recycling the Anode and Electrolyte from Spent Lithium-Ion Batteries, *ACS Sustainable Chem. Eng.*, 2020, **8**, 13527–13554.
5 N. Peeters, K. Binnemans and S. Riaño, Solvometallurgical Recovery of Cobalt from Lithium-Ion Battery Cathode Materials Using Deep-Eutectic Solvents, *Green Chem.*, 2020, **22**, 4210–4221.
6 J. Neumann, M. Petranikova, M. Meeus, J. D. Gamarra, R. Younesi, M. Winter and S. Nowak, Recycling of Lithium-Ion Batteries—Current State of the Art, Circular Economy, and Next Generation Recycling, *Adv. Energy Mater.*, 2022, **12**, 2102917.
7 X. Zhen, Z. Zhu, X. Lin, Y. Zhang, Y. He, H. Cao and Z. Sun, A Mini-Review on Metal Recycling from Spent Lithium-Ion Batteries, *Engineering*, 2018, **4**, 361–370.
8 E. Gratz, Q. Sa, D. Apelian and Y. Wang, A Closed Loop Process for Recycling Spent Lithium-Ion Batteries, *J. Power Sources*, 2014, **262**, 255–262.
9 S. Virolainen, T. Wesselborg, A. Kaukinen and T. Sainio, Removal of Iron, Aluminium, Manganese and Copper from Leach Solutions of Lithium-Ion Battery Waste Using Ion Exchange, *Hydrometallurgy*, 2021, **202**, 105602.
10 F. Peng, D. Mu, R. Li, Y. Liu, Y. Ji, C. Dai and F. Ding, Impurity Removal with Highly Selective and Efficient Methods and the Recycling of Transition Metals from Spent Lithium-Ion Batteries, *RSC Adv.*, 2019, **9**, 21922–21930.
11 C. Yu, Z. Shao, L. Liu and H. Hou, Selective Removal of Copper(II) from Aqueous Solution by a Highly Stable Hydrogen-Bonded Metal–Organic Framework, *Cryst. Growth Des.*, 2018, **18**, 3082–3088.
12 G. Aragay, J. Pons and A. Merkoçi, Recent Trends in Macro-, Micro-, and Nanomaterial-Based Tools and Strategies for Heavy-Metal Detection, *Chem. Rev.*, 2011, **111**, 3433–3458.
13 B. Zhang, H. Gao, P. Yan, S. Petcher and T. Hasell, Inverse Vulcanization below the Melting Point of Sulfur, *Mater. Chem. Front.*, 2020, **4**, 669–675.
14 J. J. Griebel, R. S. Glass, K. Char and J. Pyun, Polymerizations with Elemental Sulfur: A Novel Route to High Sulfur Content Polymers for Sustainability, Energy and Defense, *Prog. Polym. Sci.*, 2016, **58**, 90–125.
15 T. Lee, P. T. Dirlam, J. T. Njardarson, R. S. Glass and J. Pyun, Polymerizations with Elemental Sulfur: From Petroleum Refining to Polymeric Materials, *J. Am. Chem. Soc.*, 2022, **144**, 5–22.
16 W. J. Chung, J. J. Griebel, E. T. Kim, H. Yoon, A. G. Simmonds, H. J. Ji, P. T. Dirlam, R. S. Glass, J. J. Wie, N. A. Nguyen, B. W. Guralnick, J. Park, Á. Somogyi, P. Theato, M. E. Mackay, Y.-E. Sung, K. Char and J. Pyun, The Use of Elemental Sulfur as an Alternative Feedstock for Polymeric Materials, *Nat. Chem.*, 2013, **5**, 518–524.
17 Y. Zhang, K. M. Konopka, R. S. Glass, K. Char and J. Pyun, Chalcogenide Hybrid Inorganic/Organic Polymers (CHIPs): *Via* Inverse Vulcanization and Dynamic Covalent Polymerizations, *Polym. Chem.*, 2017, **8**, 5167–5173.
18 M. P. Crockett, A. M. Evans, M. J. H. Worthington, I. S. Albuquerque, A. D. Slattery, C. T. Gibson, J. A. Campbell, D. A. Lewis, G. J. L. Bernardes and J. M. Chalker, Sulfur-Limonene Polysulfide: A Material Synthesized Entirely from Industrial By-Products and Its Use in Removing Toxic Metals from Water and Soil, *Angew. Chem., Int. Ed.*, 2016, **55**, 1714–1718.
19 M. J. H. Worthington, M. Mann, I. Y. Muhti, A. D. Tikoalu, C. T. Gibson, Z. Jia, A. D. Miller and J. M. Chalker, Modelling Mercury Sorption of a Polysulfide Coating Made from Sulfur and Limonene, *Phys. Chem. Chem. Phys.*, 2022, **24**, 12363–12373.
20 M. J. H. Worthington, R. L. Kucera, I. S. Albuquerque, C. T. Gibson, A. Sibley, A. D. Slattery, J. A. Campbell, S. F. K. Alboaiji, K. A. Muller, J. Young, N. Adamson, J. R. Gascooke, D. Jampaiah, Y. M. Sabri, S. K. Bhargava, S. J. Ippolito, D. A. Lewis, J. S. Quinton, A. v Ellis, A. Johs, G. J. L. Bernardes and J. M. Chalker, Laying Waste to Mercury: Inexpensive Sorbents Made from Sulfur and Recycled Cooking Oils, *Eur. J. Chem.*, 2017, **23**, 16219–16230.
21 B. Zhang, L. J. Dodd, P. Yan and T. Hasell, Mercury Capture with an Inverse Vulcanized Polymer Formed from Garlic Oil, a Bioderived Comonomer, *React. Funct. Polym.*, 2021, **161**, 104865.
22 J. M. Chalker, M. Mann, M. J. H. Worthington and L. J. Esdaile, Polymers Made by Inverse Vulcanization for Use as Mercury Sorbents, *Org. Mater.*, 2021, **03**, 362–373.

23 D. J. Parker, H. A. Jones, S. Petcher, L. Cervini, J. M. Griffin, R. Akhtar and T. Hasell, Low Cost and Renewable Sulfur-Polymers by Inverse Vulcanisation, and Their Potential for Mercury Capture, *J. Mater. Chem. A*, 2017, **5**, 11682–11692.
24 T. Hasell, D. J. Parker, H. A. Jones, T. McAllister and S. M. Howdle, Porous Inverse Vulcanised Polymers for Mercury Capture, *Chem. Commun.*, 2016, **52**, 5383–5386.
25 A. S. M. Ghumman, M. M. Nasef, M. R. Shamsuddin and A. Abbasi, Evaluation of Properties of Sulfur-Based Polymers Obtained by Inverse Vulcanization: Techniques and Challenges, *Polym. Polym. Compos.*, 2021, **29**, 1333–1352.
26 J. M. Chalker, M. J. H. Worthington, N. A. Lundquist and L. J. Esdaile, Synthesis and Applications of Polymers Made by Inverse Vulcanization, *Top. Curr. Chem.*, 2019, **377**, 16.
27 J. Wu, R. M. Yadav, M. Liu, P. P. Sharma, C. S. Tiwary, L. Ma, X. Zou, X. D. Zhou, B. I. Yakobson, J. Lou and P. M. Ajayan, Achieving Highly Efficient, Selective, and Stable CO_2 Reduction on Nitrogen-Doped Carbon Nanotubes, *ACS Nano*, 2015, **9**, 5364–5371.
28 Z. Ren, X. Jiang, L. Liu, C. Yin, S. Wang and X. Yang, Modification of High sulfur Polymer Using a Mixture Porogen and Its Application as Advanced Adsorbents for Au(III) from Wastewater, *J. Mol. Liq.*, 2021, **328**, 11543729.
29 A. Hoefling, D. T. Nguyen, Y. J. Lee, S.-W. Song and P. Theato, A Sulfur–Eugenol Allyl Ether Copolymer: A Material Synthesized *via* Inverse Vulcanization from Renewable Resources and Its Application in Li–S Batteries, *Mater. Chem. Front.*, 2017, **1**, 1818–1822.
30 A. M. Abraham, S. V. Kumar and S. M. Alhassan, Porous Sulphur Copolymer for Gas-Phase Mercury Removal and Thermal Insulation, *J. Chem. Eng.*, 2018, **332**, 1–7.
31 N. A. Lundquist, M. J. H. Worthington, N. Adamson, C. T. Gibson, M. R. Johnston, A. V. Ellis and J. M. Chalker, Polysulfides Made from Re-Purposed Waste Are Sustainable Materials for Removing Iron from Water, *RSC Adv.*, 2018, **8**, 1232–1236.
32 X. Wu, J. A. Smith, S. Petcher, B. Zhang, D. J. Parker, J. M. Griffin and T. Hasell, Catalytic Inverse Vulcanization, *Nat. Commun.*, 2019, **10**, 647.
33 J. Chalker and M. Mann, *Materials and Processes for Recovering precious metals*, 2020.
34 N. G. Mbewana-Ntshanka, M. J. Moloto and P. K. Mubiayi, Role of the Amine and Phosphine Groups in Oleylamine and Trioctylphosphine in the Synthesis of Copper Chalcogenide Nanoparticles, *Heliyon*, 2020, **6**, e05130.
35 X. Liu, M. Atwater, J. Wang, Q. Dai, J. Zou, J. P. Brennan and Q. Huo, A Study on Gold Nanoparticle Synthesis Using Oleylamine as Both Reducing Agent and Protecting Ligand, *J. Nanosci. Nanotechnol.*, 2007, **7**, 3126–3133.
36 S. Mourdikoudis and L. M. Liz-Marzán, Oleylamine in Nanoparticle Synthesis, *Chem. Mater.*, 2013, **25**, 1465–1476.
37 W. Xuan, A. Otsuki and A. Chagnes, A. Investigation of the Leaching Mechanism of NMC 811 ($LiNi_{0.8}Mn_{0.1}Co_{0.1}O_2$) by Hydrochloric Acid for Recycling Lithium-Ion Battery Cathodes, *RSC Adv.*, 2019, **9**, 38612–38618.
38 X. Xiao, B. W. Hoogendoorn, Y. Ma, S. Ashoka Sahadevan, J. M. Gardner, K. Forsberg and R. T. Olsson, Ultrasound-Assisted Extraction of Metals from Lithium-Ion Batteries Using Natural Organic Acids, *Green Chem.*, 2021, **23**, 8519–8532.
39 J. L. Zhang, R. S. Srivastava and R. D. K. Misra, Core−Shell Magnetite Nanoparticles Surface Encapsulated with Smart Stimuli-Responsive Polymer: Synthesis, Characterization, and LCST of Viable Drug-Targeting Delivery System, *Langmuir*, 2007, **23**, 6342–6351.
40 N. Shukla, C. Liu, P. M. Jones and D. Weller, FTIR Study of Surfactant Bonding to FePt Nanoparticles, *J. Magn. Magn. Mater.*, 2003, **266**, 178–184.
41 A. Gupta, M. J. H. Worthington, H. D. Patel, M. R. Johnston, M. Puri and J. M. Chalker, Reaction of Sulfur and Sustainable Algae Oil for Polymer Synthesis and Enrichment of Saturated Triglycerides, *ACS Sustainable Chem. Eng.*, 2022, **10**, 9022–9028.
42 J. W. Thomson, K. Nagashima, P. M. Macdonald and G. A. Ozin, From Sulfur−Amine Solutions to Metal Sulfide Nanocrystals: Peering into the Oleylamine−Sulfur Black Box, *J. Am. Chem. Soc.*, 2011, **133**, 5036–5041.
43 H. B. Abrahamson, A. B. Rezvani and J. G. Brushmiller, Photochemical and Spectroscopic Studies of Complexes, of Iron(III) with Citric Acid and Other Carboxylic Acids, *Inorg. Chim. Acta*, 1994, **226**, 117–127.